

Performance improvement of earthquake-resistant steel structure system EBF (Eccentrically Braced Frame) by using modified long links

Maiyozzi Chairi^{1*}, Zaidir², Sabril Haris³, and Yurisman⁴

¹Civil Engineering Doctoral Student, Universitas Andalas, Indonesia

^{2,3}Civil Engineering Department, Universitas Andalas, Indonesia

⁴Civil Engineering Department, Politeknik Negeri Padang, Indonesia

Abstract. This paper presents the results of a numerical study of the behavior of paired Long links in a modified EBF portal. The aim of the research is to examine the behavior of Long links and their EBF portals numerically against the parameters that influence the behavior of Long links and obtain behavior that approaches the performance of short links according to AISC-341 loading standards. The analysis uses a finite element approach MSC/NASTRAN 2023. The portal is modeled as a shell element supported at the base of the column, lateral loading is carried out at the left end of the beam-column junction (x-axis). While the link element is modeled as a shell element supported at both ends, several nodes in the loading position are allowed to translate in the y-axis direction. The analysis results show the parameters of web thickness, and flange thickness, along with the thickness and geometric stiffeners. Several modeled link types can improve Long-link performance in terms of strength, stiffness, and energy dissipation. However, significant results have not yet been obtained regarding the performance of long links which are close to the performance of sliding links.

1 Introduction

In the last two decades, there have been many earthquakes in many countries in the world. The earthquake has caused loss of life and property. The amount of damage and losses caused by earthquakes will likely increase in the future. Many of the buildings that were built did not follow the basic principles of earthquake-resistant buildings, and even the quality of the materials and workmanship was so low that the possibility of damage and collapse of these buildings was very large, even though the intensity of the earthquake was not too large. Indonesia has a history of earthquakes because Indonesia is in the Ring of Fire region (an area that frequently experiences volcanic eruptions and earthquakes), the biggest being the Aceh earthquake on 25 December 2004 with a magnitude of 9.1-9.3 on the Richter scale. Based on the latest Indonesian National Standard (SNI) for Earthquakes (1726-2019) concerning procedures for planning earthquake resistance for building and non-building structures, earthquake-resistant building structures are generally planned by applying the concept of ductility [1]. That is by selecting certain structural elements, which are designed and expected to experience plastification (damage) in the event of a strong earthquake. The structure is expected not to collapse, by

planning certain elements of the structure so that they can experience stable inelastic deformation during strong earthquakes.

Steel structures are very good at carrying earthquake loads because steel materials have higher strength and ductility when compared to other structural materials (e.g. concrete). Currently, 3 types of earthquake-resistant steel structural systems are commonly used, namely moment-resisting frame systems, concentrically braced frames, and eccentrically braced frames. The eccentrically braced frame (EBF) is considered to be a good resister to seismic forces due to the combination of great ductility and high stiffness [2, 3]. The EBF system resists lateral loads through a combination of frame and truss action. In other words, it can be seen as a hybrid system between Moment Resisting Frame (MRF) and Concentrically Braced Frame (CBF). EBF provides high ductility like MRF with a concentration of inelastic action on the links, and at the same time provides a level of elastic stiffness similar to that provided by CBF [4, 5, 6]. The link structure element acts as a fuse in the EBF structure which is planned to behave inelastically under extreme loading conditions.

* Corresponding author: maiyozzi@upiyptk.ac.id

2 Objectives

The purpose of this study is to obtain the maximum performance of the EBF structure and approach the performance of the short link by increasing the performance of the link elements, in this case, the long link is used. To achieve this, this study aims to 1) Obtain numerical link behavior for parameters that significantly influence the Long link in the EBF system, 2) Obtain the performance of the Long link numerically as a separate component, and as part of the EBF system and approach the performance short link.

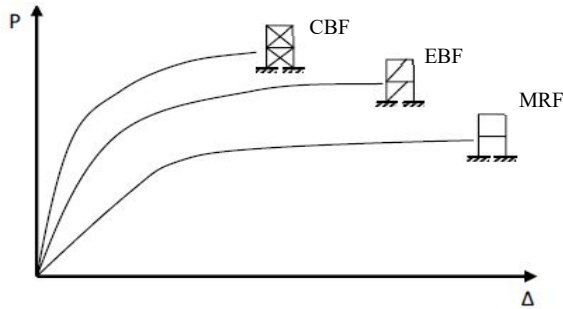


Fig. 1. Differences in the behavior of the three models of steel structural systems [7, 8, 9].

3 Literature Review

3.1 Previous research on the EBF system

In the 1970s to 1980s, EBF has been used as the frame system of choice in areas of high seismicity [4-6, 10, 11]. Studies on the behavior of EBF systems have started since the 1970s ((continued into the 1980s).

In 2010, Yurisman et al conducted a study on shear/short links using diagonal stiffeners on the web. Important parameters for the shear link behavior are flange thickness, web thickness, stiffener thickness, spacing, thickness of the diagonal stiffeners, and geometric of the diagonal stiffeners [9]. The behavior of shear links with web diagonal stiffeners was then compared with standard links [12]. The results show that the web diagonal stiffener can improve the performance of the shear link in terms of strength, stiffness, and energy dissipation in resisting lateral loads. However, ductility performance did not get such significant results. The results of the analysis also show that the thickness of the diagonal stiffener and the geometric model of the stiffener have a significant effect on the performance of the shear link.

In 2017, Abdelkarim et al conducted research on steel links made using several longitudinal stiffeners in a web plate that allow for the overall plate buckling behavior [13]. The program is numerically and experimentally carried out. The ductility while cyclic was studied and compared at different stiffener geometries. Thus the result of applying flexible stiffeners offers a high bending resistance of the web and increases ductility. And the

optimal stiffener Geometry can be found to achieve moderate to high ductility.

3.2 Overview of the EBF seismic steel structure system

The eccentrically braced frame structure system (EBF) is the development of two existing lateral force-resisting structural systems: MRF and CBF. This system was developed to improve the MRF and CBF systems, where the MRF system has a large and stable value of ductility and energy dissipation capacity but has a relatively low stiffness value, on the other hand, CBF has greater stiffness but has a lower energy dissipation capacity. Figure 1 shows the differences in the behavior of the three models of steel structure systems while Figure 2 shows several forms of EBF systems that are commonly used [14].

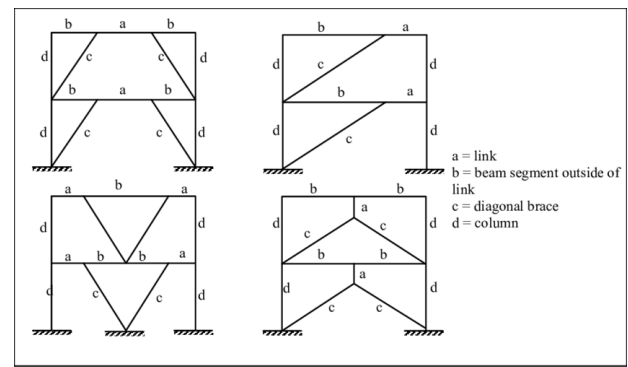


Fig. 2. Configurations of eccentrically braced frames [14].

In the EBF system, seismic energy absorption is carried out through the mechanism of forming plastic hinges on the link elements. The link element is a part of the beam designed to dissipate energy in the event of a strong earthquake. The yield that occurs in the link elements can be either shear or bending. This type of yielding is highly dependent on the length of the link.

3.3 Characteristics of the link element

The experimental results show that the inelastic deformation capacity of an EBF can be greatly reduced when long links ($e > e_0$) are used. It can be shown that the bending hinge dominates the response of the link when e is greater than $2.6 M_p/V_p$, (If the moment at the bending hinge is $1.2M_p$, the corresponding shear for a link of that length is $0.92V_p$). In the transition region where $1.6M_p/V_p < e < 2.6M_p/V_p$ the link undergoes shear and bending results simultaneously [15]. Figure 3 Classify results

For design purposes, a link is classified as short or shear, long, or intermediate. The link length affects the failure mode and deformation capacity [16]. The link rotation angle is the plastic rotation angle between the link and the beam portion outside the link. Tests show that the inelastic link rotation capacity depends on the link length. The shorter, the greater the rotational capacity [4, 5]. To develop a large rotational capacity, it is necessary to have

intermediate links with closely spaced stiffeners. The allowable link deformation capacity, ∇a , is given by AISC 341 (2010) [12].

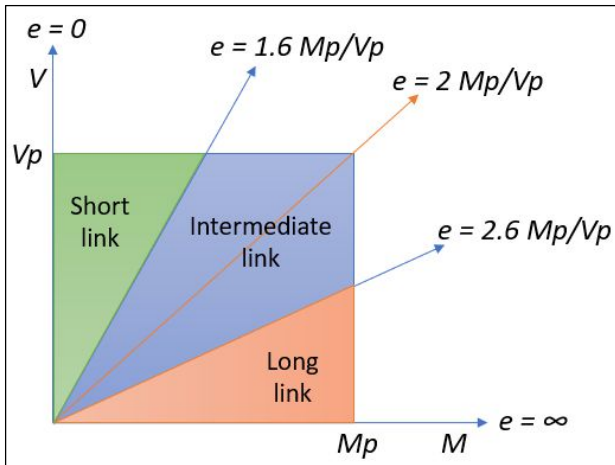


Fig. 3. Classification of links, modified of Bruneau 2011 [17].

The link is said to be a shear link if the yielding that occurs is caused by a shear force and is said to be a bending link if the yielding that occurs is caused by a bending moment. Post-bending deformation of a link beam is caused by: shear yielding, bending yielding, or a combination of both. By using a simple analytical model it is possible to determine an exact boundary between the bending mechanism and the shear mechanism. This limitation can be described using a shear stretch that yields simultaneously under bending and shear conditions [18].

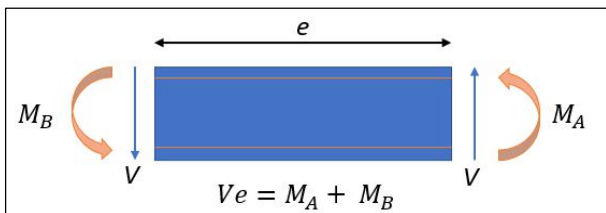


Fig. 4. Link deformation and free-body diagram, modified of Bruneau 2011 [17].

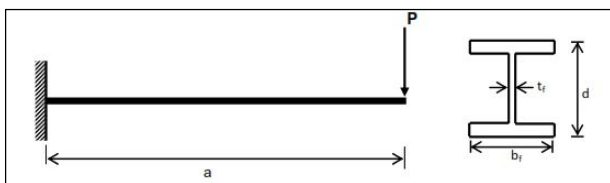


Fig. 5. Shear spans and simple cantilever beam sections [7, 8, 9].

Shear span is the ratio between the moment and the shear at a point or the distance between the point $M = 0$ (inflection point) and the maximum moment point where there is no additional load between the two points. The behavior of the links in the EBF system under mechanism conditions is described by the same concept of a simple shear stretch as in Figure 4. A balanced strength ratio (balance strength ratio) is achieved when the shear stretch experiences bending yielding and shearing

simultaneously. Shear stretches in their simplest form are depicted as cantilever beams that are loaded at the ends, as shown in Figure 5.

$$a = \frac{M}{V} \quad (1)$$

Where a = shear span length of the cantilever beam, M = moment acting on the beam, V = shear force acting on the beam. Meanwhile, the length of the cantilever under balanced strength conditions is expressed by the formula:

$$a_b = \frac{M_p}{V_p} \quad (2)$$

where :

$$M_p = Z_x \cdot F_y \quad (3)$$

$$V_p = 0.6 \cdot F_y \cdot d \cdot t_w \quad (4)$$

Where a_b = strength ratio in balanced condition (balance strength ratio). M_p = plastic moment, V_p = plastic shear force, Z_x = x-direction section modulus, d = height of WF profile beam, t_w = thickness of WF profile web, F_y = yield stress of steel material. The cantilever beam will yield due to shear if the cantilever length is less than a_b and will yield due to bending if the cantilever length exceeds a_b . From the perspective of the design criteria the link is considered as a beam that is restrained at both ends, the link length in a balanced condition is expressed by the formula:

$$e_b = 2 \cdot a_b = 2 \cdot \frac{M_p}{V_p} \quad (5)$$

where : e_b = balance link length

Based on the yielding mechanism that occurs in the link beam, the links are divided into two types, namely: a link that yields due to moments is called a bending link, and a link that yields due to shear is called a shear link. However, there is no clear demarcation between flexural yielding and shear yielding. Identifying a yielding link due to bending or shear can be done through tests. The pure shear condition is considered to occur when the link length (e) is a maximum of 80% of the shear span length in the balanced condition (e_b). So $e \leq 80\% e_b = 0.8 \cdot 2a_b = 1.6M_p/V_p$. Meanwhile, pure bending conditions are considered to occur when the link length (e) is more than $5M_p/V_p$. The behavior of the link beam between the two conditions is described using the strength ratio M_p/V_p as follows: 1) pure shear link if: $e < 1.6M_p/V_p$, 2) shear dominant link if $1.6M_p/V_p < e < 2.6M_p/V_p$, 3) dominant flexural link if: $2.6M_p/V_p < e < 5.0M_p/V_p$, 4) pure flexural link if: $e > 5M_p/V_p$.

For very short links the link shear force reaches a plastic shear capacity $V_p = 0.55 \cdot h_w \cdot t_w \cdot F_y$ and the yielding link due to shear forms a shear hinge. For longer links, the end moment reaches M_p forming the flexural joints before shear yielding occurs. The differences between the failure

modes of the shear link and the flexural link are shown in Figure 6.

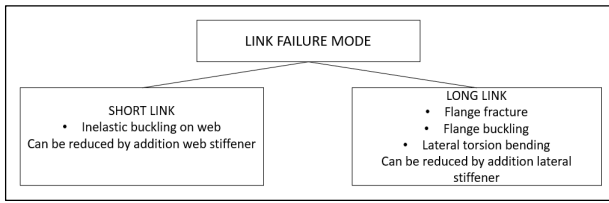


Fig. 6. Differences in flexural (long) and shear (short) link failure modes.

4 Numerical Study of Long Link Performance

4.1 Preliminary analysis

In the results of the literature study, it was concluded that short links are the most efficient links used in EBF. The initial analysis was carried out numerically using finite elements using the NASTRAN 2023 programming application. Further research was carried out using long links with several changes and modifications to the links. From several studies, long links have smaller deformation angles than short links but have smaller ductility and energy dissipation values. And from an architectural point of view, the installation of a longer link will provide a wider space to be utilized as open areas such as doors and windows.

The profile used in the EBF portal is 150.100.6.9 for beam, link, and bracing elements. And the profile 200.100.5,5.8 on the column. The thickness of the stiffeners in each model is made the same, namely $t_s : 8$ mm. The parameter study used for long links is planned using steel profiles IWF 150.100.6.9 with the calculations:

$$M_p = Z_x \cdot F_y \quad (6)$$

$$F_y = 240 \text{ Mpa}$$

$$Z_x = 1,12 \text{ Sx} = 1,12 \times 138.000 = 154.560 \text{ mm}^3$$

$$M_p = 240 \times 154.560 = 37.094.400 \text{ N mm}$$

$$V_p = \sigma_y \cdot Atw \quad (7)$$

$$\sigma_y = 0,6 \times F_y = 144$$

$$Atw = (d - 2 \cdot tf) \cdot tw \quad (8)$$

$$32 \cdot 6 = 792 \text{ mm}^2$$

$$V_p = 144 \cdot 792 = 114.048 \text{ N}$$

Estimates for lg link: Length ratio is used = 2,65

$$\frac{2,65 M_p}{V_p} \quad (9)$$

$$\frac{2,65 (37.094.400)}{114.048} = 861,91 \text{ mm} = 86,19 \text{ cm} \sim 86 \text{ cm (link length)}$$

Tensile test material data was used, taken based on material data in previous studies [9]. With $E = 200,000$ MPa, $F_y = 240$ MPa, and a Poisson ratio = 0.3. The curve used uses true stress-strain. After the tensile test, the value obtained becomes $F_y = 300$ Mpa are shown in Figure 7.

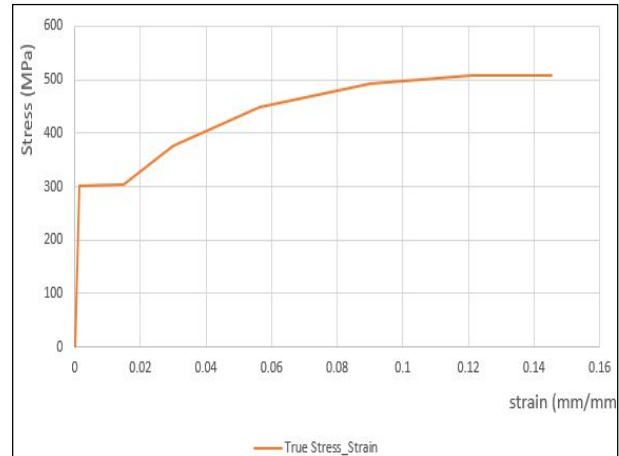


Fig. 7. Tensile test curve (stress/strain).

As for the loading standards used based on AISC-341 [12]. The standard loading model given to the test object is adjusted to the loading sequence, where the load given to the test object is determined by the total link rotation angle.

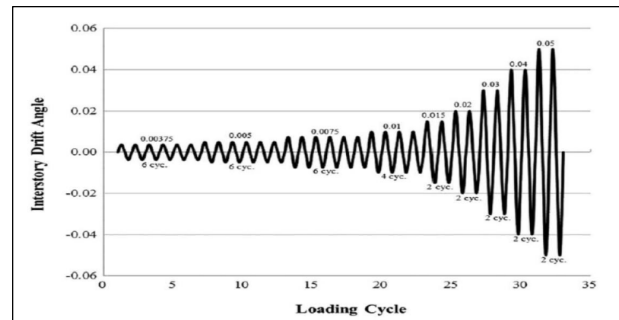


Fig. 8. Loading protocol on the EBF portal [12].

4.2 Long link finite element modeling

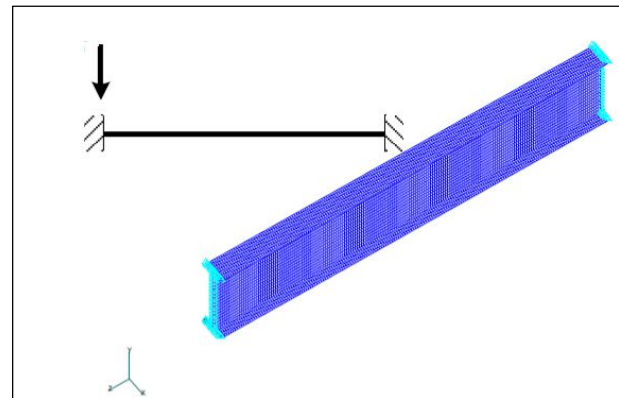


Fig. 9. Long link finite element modeling.

The link is modeled as a shell element that is supported at both ends while some nodes at the loading position are allowed to translate in one direction only (y-direction). As an approach to the forces acting on the link, one end of the link is modeled as a fixed element, while the other end is modeled as a fixed element but given the freedom to move in the transverse direction.

Whereas in the EBF system, it is modeled as a portal that is fixed on the support (column base) and is given a lateral force at the joint of the column beams.

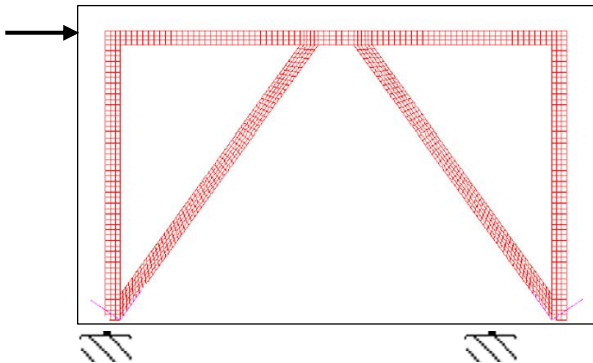


Fig. 10. EBF modeling used (K-EBF).

The flow chart in Figure 11 shows the steps to be carried out in a numerical assessment of long-link behavior and performance.

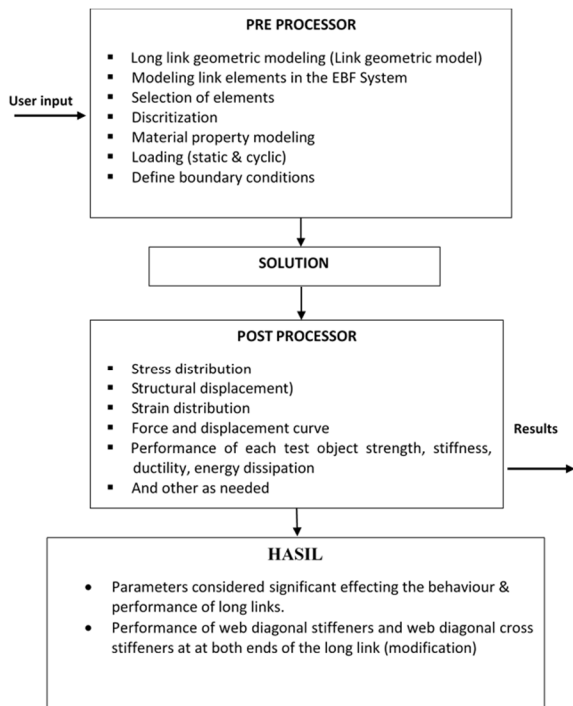


Fig. 11. The assessment phase is carried out numerically on long link performance.

4.3 Parameters that affect the performance of long links

The results of the initial study show several parameters that affect the performance of the long link, namely: Sectional parameters include: flange thickness (flange) and web thickness (web) and Stiffener parameters include: stiffener thickness and stiffener spacing.

Parameters of the effect of body thickness and wing thickness showed significant results. This means that the slenderness of the section affects the occurrence of local buckling on the flange and the web of the profile. In other

words, the thicker the body or wings, the greater the acceptable force. Figure 12 and Figure 13 show the effect of section slenderness on the performance of the long link test object model.

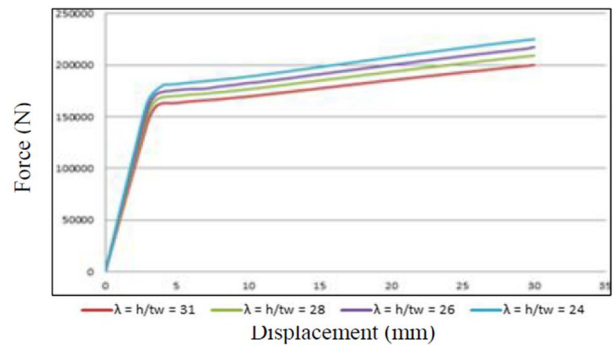


Fig. 12. Effect of web thickness (t_w).

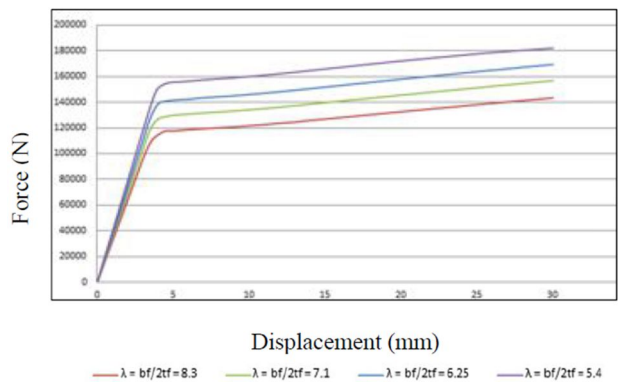


Fig. 13. Effect of flange thickness (t_f).

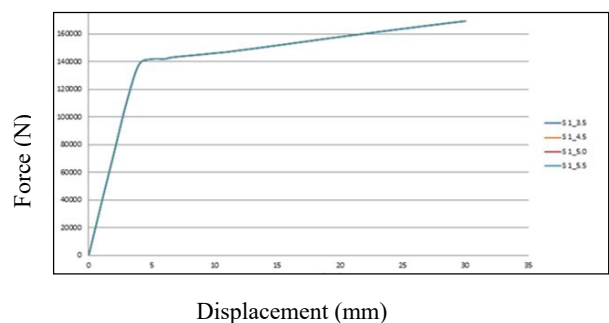


Fig. 14. Effect of stiffener thickness.

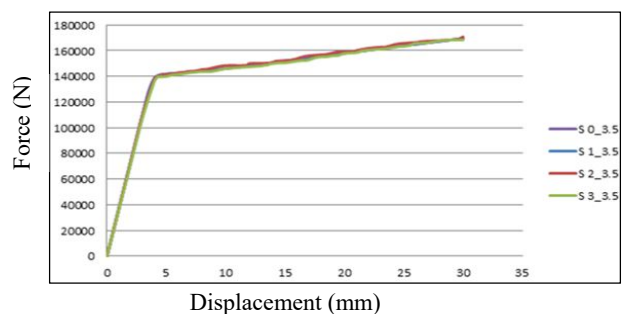


Fig. 15. Effect of stiffener distance.

While the parameters of stiffener thickness and vertical stiffener distance did not show significant results. This means that the existence of a vertical stiffener does not affect the performance of the long link, especially in elastic conditions, it can be seen that the four curves coincide with each other. Figure 14 and Figure 15 show the effect of stiffener thickness and stiffener distance.

4.4 Behavioral trends of the long link element and the portal of the long link element (EBF)

Calculations between the Long link element model (sub-assembly) and the link model used in an EBF portal system yield results and curve trends that are not much different. The difference is that the curve model shown in the EBF portal is more plastic than the Long link element. This shows that even when carrying out tests and calculations in the form of elements or the form of Portals, this is interpreted to represent the behavior of the Long link. By the finite element settings in each model used. The results can be seen in the curves of Figure 16 and Figure 17.

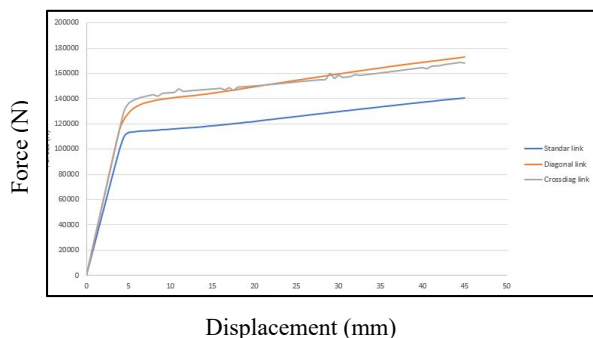


Fig. 16. Long link element curve.

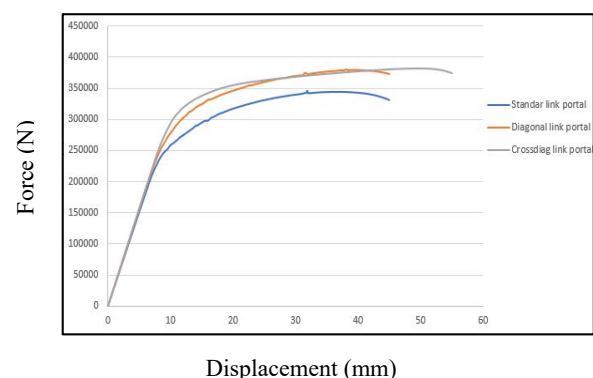


Fig. 17. EBF long link portal element curve.

4.5 The effect of long link model variations

Based on the results of preliminary studies that have been carried out numerically, several indications were found in the form of the effect of thickness on the wing and web, while the effect of stiffener distance and vertical thickness of the stiffener does not affect the performance of the long link. Therefore the author tries to give a variation to the Long link with the addition of a diagonal stiffener (this is based on previous research that was tested for increased

performance on short/shear links), and also tries other variations with the addition of two diagonal stiffeners.

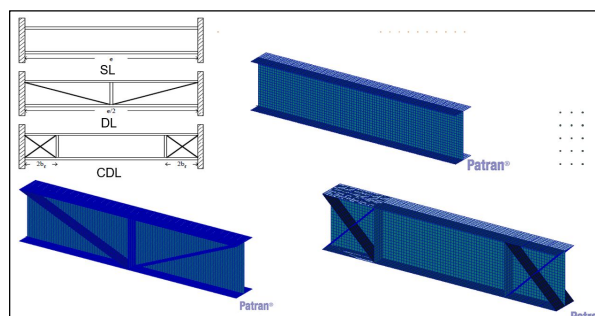


Fig. 18. Variations in the model of the link specimens used.

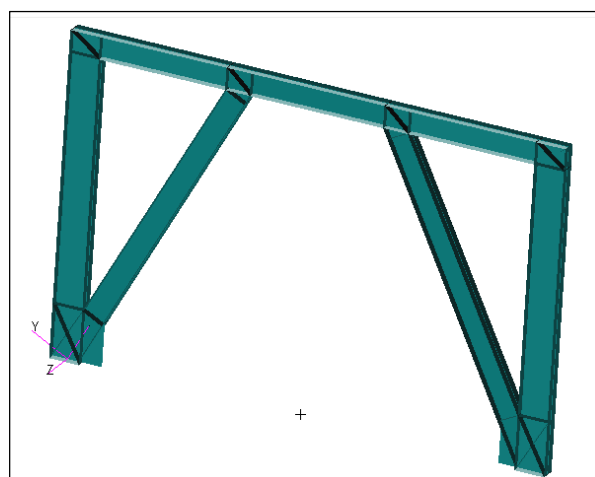


Fig. 19. Portal specimens model (EBF).

Indicators of the ability of the long link to withstand lateral forces (link behavior) and the ability to dissipate energy can be expressed in the form of a force vs. displacement curve from a static monotonic loading and a hysteretic curve for a force vs. displacement from a cyclic loading result.

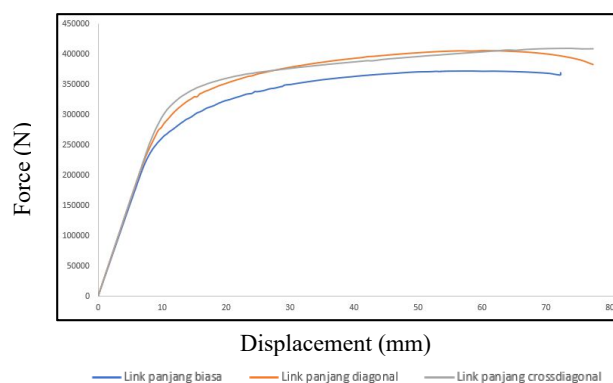


Fig. 20. The effect curve of the variation of the link specimen models used.

The load-displacement curve in Figure 20 shows that the variation of the Long link model has a significant influence on the performance of the Long link. However, under elastic conditions, it can be seen that the three curves in each model coincide with each other. Meanwhile, the Long link model with cross-diagonal

stiffeners shows good performance in inelastic conditions and is almost the same as the Long link with diagonal stiffeners. The first yielding varies when the load-displacement $dy = 7.34$ mm, $dy = 7.97$ mm, and $dy = 8.39$ mm.

Table 1. Comparison of the behavior of long link model variations.

Portal Models	Standard Portal link (SL)	Diagonal Portal link (DL)	Crossdiagonal Portal link (CDL)
dy (mm)	7.34	7.97	8.39
du (mm)	63.64	61.92	64.93
Py (N)	219669.48 57	243262.6841	260627.8649
Pu (N)	371145.93 95	405317.6949	405814.8816
μ (daktilitas)	8.6702997 28	7.769134253	7.73897497
K. Elastis (N/mm)	29927.722 85	30522.29412	31064.10785

4.6 Energy dissipation

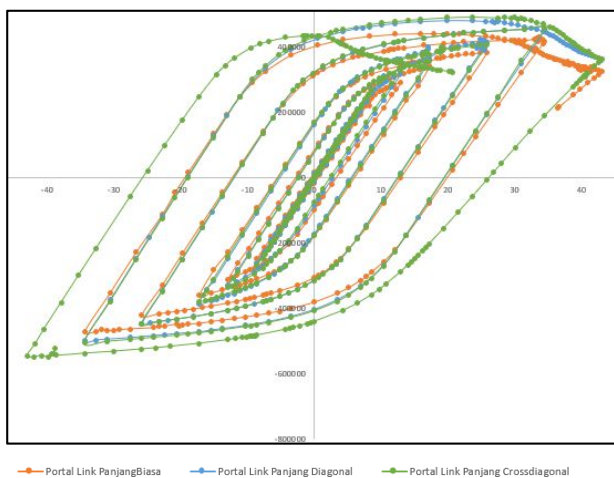


Fig. 21. The hysteretic curve affects the variation of the link specimen models used.

One of the important parameters for measuring the performance of structures in resisting earthquake forces is the ability to dissipate energy. In an earthquake-resistant steel structure system of the EBF type, earthquake energy dissipation occurs through a plastification process in the link elements. The energy dissipation value is obtained from the hysteretic curve which states the connections between force and displacement. The hysteretic curve is obtained from the results of testing the cyclic loading pattern which can be done numerically or experimentally. The cyclic loading protocol used in this study refers to the loading protocol stipulated by the standard AISC-341 as shown in Fig. 8. Tests with cyclic loading patterns were

carried out on a variety of specimen models: standard portal models (AISC standard long links), diagonal portals (diagonal long links), and cross-diagonal portals (cross diagonal long links). The hysteretic curve shown in Figure 21 generally shows that the three specimen models obtain energy dissipation capacity values that are not much different (not significant). However, with the same analysis, the curve of the test object model with cross-diagonal links has an advantage of one cycle compared to the other 2 models. In previous research, the energy dissipation ability can be further increased by increasing the thickness of the stiffener. Therefore, it is necessary to consider the model of the link and the thickness of the stiffener to optimally increase all these parameters.

5 Conclusion

Important parameters related to the performance of an earthquake-resistant system are strength, stiffness, ductility, and energy dissipation value. With these parameters, the ability of a structure to dissipate seismic energy can be measured. The values of strength, stiffness, and ductility can be seen as shown in Table 1, while the ability of the specimen models to dissipate energy is reflected in the area of the hysteretic curve produced by cyclic loading. Based on the results of a numerical study of several seismic parameters that are considered to affect long-link performance, it can be concluded as follows :

1. Parameters of the effect of web thickness and flange thickness showed significant results. This means that the slenderness of the cross-section is quite influential on the occurrence of local buckling on the flange and the web of the profile. The thicker the web or flange, the greater the acceptable force. The effect of cross-sectional slenderness on the performance of the Long-link specimen models can be seen in Figure 12 and Figure 13.
2. The thickness of stiffeners and distance of lateral stiffeners attached to the link web have no significant effect on the seismic behavior of the link. In the sense that the existence of a vertical stiffener does not affect the performance of the long link, especially in elastic conditions, it can be seen that the four curves coincide with each other as shown in the curve of Figure 14.
3. The variation of the Long link model has a significant effect on the performance of the Long link. However, under elastic conditions, it can be seen that the three curves in each model coincide with each other. Meanwhile, the Long link model with cross diagonal stiffeners shows good performance under inelastic conditions and is almost the same as the Long link with diagonal stiffeners as shown in the displacement load curve in Figure 20. The first yielding varies when the load displacement is $dy = 7.34$ mm, $dy = 7.97$ mm, and $dy = 8.39$ mm as shown in Table 1.
4. The hysteretic curve in Figure 21 generally shows that the three models of specimens obtain energy dissipation capacity values that are not much different (not significant). However, with the same analysis, the

curve of the specimen model with cross diagonal links has an advantage of one cycle compared to the other 2 models. In previous research, the energy dissipation ability can be further increased by increasing the thickness of the stiffener. Therefore, it is necessary to consider the model of the link and the thickness of the stiffener to optimally increase all these parameters.

References

1. National Standardization Agency. SNI 1726-2019. Earthquake Resistance Planning Procedures for Building and Non-Building Structures, **8**, 254 (2019)
2. A. Ghobarah, T. Ramadan, JCE, 140-148 (1991)
3. J. M Binder,. Gray, C de Oliveira, Cast Steel Replaceable Modular Links for Eccentrically Braced Frames, ASCE SC/ University of Exeter on 04/04/17 (2017)
4. E. P. Popov, Journal of Engineering Structures. **5(1)** : 3-9 (1983)
5. K. Kasai, E. P. Popov. JSE, **112 (3)**, 505–523. (1986)
6. K. Kasai, E. P. Popov. JSD. Vol **112**, No.2:362-382. February, ASCE (1986)
7. Yurisman, B. Budiono, M. Mustopo, S. Made, Behavior of sliding links with body diagonal stiffeners on eccentric supported steel frame structure systems (EBF), Seminar Nasional PMPMBIK, Universitas Katolik Parahyangan Bandung (2009)
8. M. Moestopo, M. Aulia, Link Performance with Bolt Joints on Eccentric Stiffened Frame Structure, Seminar HAKI, Agustus, Jakarta (2006)
9. Yurisman, B. Budiono, M. Moestopo, M. Suarjana, M. N. JTS, **17(1)**, 25. (2010)
10. J. O. Malley, E. P. Popov, JSE, **110 (9)**, 2275–2295. (1984)
11. J. M. Ricles, E. P. Popov, JSE, **115(8)**, 2046–2066. (1989)
12. AISC 341-10 - American Institute of Steel Construction. Seismic Provisions for Structural Steel Buildings, 1, 402 (2010)
13. A. Dib, L. G. Vigh, PE, **196** (June), 82–89 (2017)
14. AISC. Seismic Provisions for Structural Steel Buildings, AISC, Inc (2005)
15. M. D. Engelhardt, E. P. Popov, JSE, **118** (11), 3067–3088. (1992)
16. T. Okazaki, Seismic Performance of Link-to-column Connections in Steel Eccentrically Braced Frames (Ph.D. Thesis) Department of Civil Engineering, UTA, Austin, TX (2004)
17. M. Bruneau, C. M. Uang, A. Whittaker, Ductile Design of Steel Structures, McGraw-Hill. (2011)
18. R. Englekirk, Steel Structures: Controlling Behaviour Through Design, JWS, Inc. (1994)